



Numerical simulation of ground and groundwater factors affecting NMR probe

Rui Deng^a, DongWu^b, Shuzheng Zhao^{c,*}

^aKey Lab of Exploration Technologies for Oil and Gas Resources, Ministry of Education (Yangtze University), Wuhan 430100, China, Tel. +86 18627807056; email: dengrui@yangtzeu.edu.cn

^bR&D Academy of Well Logging Technologies, CNPC Greatwall Drilling Company, Beijing 102200, China, Tel. +86 13942765472; email: 732677035@qq.com

^cTianjin Branch, CNOOC (China) Co., Ltd., Tianjin 300452, China, Tel. +86 15822613669; email: dunray@163.com

Received 26 February 2018; Accepted 10 April 2018

ABSTRACT

With the development of science and technology, nuclear magnetic resonance (NMR) phenomenon has been studied. It has already entered the stage of application and development by theoretical research and test. In addition, it has also been widely used in geoscience (proton magnetometer, NMR spectrometer, core testing instrument and NMR logging). On the basis of this, the NMR technique is proposed to detect the numerical simulation of groundwater. The simulation model of layered earth aquifer is established. The simulation results show that the water content of the aquifer, the change of the area of the coil and the depth of the aquifer all have some influence on the NMR signal. That is, the same NMR signal tested on the ground may be the response of the aquifer with the same depth, different thickness and water content on the ground. This also means that the measured data in one location in the field can be retrieved into the results of different stratigraphic models.

Keywords: NMR; Numerical simulation; Aquifer

1. Introduction

Using ground nuclear magnetic resonance (SNMR) detecting the underground art technology is the study of a certain depth of the formation. It is excited proton NMR signal, only advantage of this approach is the formation in order to detect the NMR signal contains water, the strength of the signal directly related to the number of hydrogen protons in water, that is, the initial amplitude of the measured NMR signal is proportional to the formation of free water content [1]. The initial amplitude of the signal is a sinusoidal oscillation and an exponential function of the change, how to calculate the NMR signal of the oscillation integral kernel few problems discussed in the literature. Further the depth, and thickness and area on the ground and the NMR signal detected in the formation water content of the aqueous layer antenna element

is how a correspondence relationship, require detailed theoretical analysis and calculation, it is in this paper proposed the case of looking for water SNMR detailed theoretical analysis, to find the actual practice of establishing a suitable ground water to find water model, the calculation method of the NMR signal is given, factors affecting the NMR signal, thereby to find the actual service water practice and provide a theoretical basis for the development of the instrument.

2. Basic theory of electromagnetic field calculation

2.1. Time and frequency domain Maxwell equations

An electromagnetic field can be used within the domain of the vector function (\vec{E}) four electric field strength, magnetic flux density (\vec{B}), electric displacement (\vec{D}), the magnetic field strength to determine (\vec{H}), all of the electromagnetic

* Corresponding author.

Presented at the 3rd International Conference on Recent Advancements in Chemical, Environmental and Energy Engineering, 15–16 February, Chennai, India, 2018.

phenomena obey Maxwell's equations [2]. Maxwell's equations in the time domain, we have the following form:

$$\begin{aligned} \nabla \times \bar{E} &= -\frac{\partial \bar{B}}{\partial t} \\ \nabla \times \bar{H} &= \bar{J}_0 + \frac{\partial \bar{D}}{\partial t} \\ \nabla \cdot \bar{B} &= 0 \\ \nabla \cdot \bar{D} &= \rho \end{aligned} \quad (1)$$

where \bar{J}_0 is the current density, ρ is the charge density.

Eq. (1) is a group of about five vectors \bar{E} , \bar{H} , \bar{B} , \bar{D} and \bar{J}_0 are mutually independent differential equations. The equation of state can be described by the relationship between the field vectors mentioned in Eq. (2) linking them.

Maxwell's equations in the time domain (Eq. (1)) are used to make a one-dimensional Fourier transform, and use the equation of state:

$$\begin{aligned} D &= \epsilon E \\ B &= \mu H \\ J &= \sigma E \end{aligned} \quad (2)$$

To obtain frequency-domain Maxwell equations:

$$\begin{aligned} \nabla \times E + i\mu\omega H &= 0 \\ \nabla \times H - (\sigma + i\epsilon\omega)E &= 0 \end{aligned} \quad (3)$$

The introduction of impedance rate $\hat{z} = i\mu\omega$. And admittivity $\hat{y} = \sigma + i\epsilon\omega$. The concept of Eq. (3) can be written as:

$$\begin{aligned} \nabla \times E + \hat{z}H &= 0 \\ \nabla \times H - \hat{y}E &= 0 \end{aligned} \quad (4)$$

2.2. Wave equation

Eq. (1) are curl:

$$\begin{aligned} \nabla \times (\nabla \times E) + \nabla \times \left(\frac{\partial b}{\partial t} \right) &= 0 \\ \nabla \times (\nabla \times h) + \nabla \times \left(\frac{\partial d}{\partial t} \right) &= \nabla \times j \end{aligned} \quad (5)$$

The equation of state of generation of the time domain into the above equation simplifies to do, to give electric and magnetic fields of the wave equation in the time domain:

$$\begin{aligned} \nabla^2 e - \mu\epsilon \frac{\partial^2 e}{\partial t^2} - \mu\sigma \frac{\partial e}{\partial t} &= 0 \\ \nabla^2 h - \mu\epsilon \frac{\partial^2 h}{\partial t^2} - \mu\sigma \frac{\partial h}{\partial t} &= 0 \end{aligned} \quad (6)$$

Of Eq. (6) taking a Fourier transform, to obtain the wave equation in the frequency domain:

$$\begin{aligned} \nabla^2 E + (\mu\epsilon\omega^2 - i\mu\sigma\omega)E &= 0 \\ \nabla^2 H - (\mu\epsilon\omega^2 - i\mu\sigma\omega)H &= 0 \end{aligned} \quad (7)$$

Assuming $k^2 = \mu\epsilon\omega^2 - i\mu\sigma\omega$, the frequency domain wave equation was written as:

$$\begin{aligned} \nabla^2 E + k^2 E &= 0 \\ \nabla^2 H - k^2 H &= 0 \end{aligned} \quad (8)$$

k is called a wave number, before the displacement current is corresponding to the entry, the entry corresponding to the current conduction. When the frequency is less than 105 Hz, there are the earth medium $\mu\epsilon\omega^2 \ll \mu\sigma\omega$. Displacement current far smaller the conduction current, the electromagnetic field at this time is mainly determined by conducting current, wave number $k \approx (-i\mu\sigma\omega)^{1/2}$. When the frequency is greater than 109 Hz, the displacement current is much greater than the conduction current, the electromagnetic field at this time is mainly determined by the displacement current, wave number $k \approx (-i\mu\sigma\omega^2)^{1/2}$.

Maxwell's equations in the frequency domain (Eq. (4)) is the homogeneous equations for the passive region, the active region to be used in the following non-homogeneous equation [6] in place:

$$\begin{aligned} \nabla \times E + \hat{z}H &= -J_m^s = -i\mu_0\omega M^s \\ \nabla \times H - \hat{y}E &= J_e^s = i\omega P^s \end{aligned} \quad (9)$$

among them J_m^s is the magnetic flux density (the amount of introduced for convenience of discussion); J_e^s is the current density. Born et al. [7] introduces a potential function, its derivative to give E and H . Potential function represented by H and E is an effective way of solving Maxwell's equations, because the potential function is consistent with the direction of the source, the potential function equation is easier than the field strength equation. Export potential function is given below.

In each homogeneous segment, the electric field and magnetic field are regarded as superposition of the field generated by the power source and the magnetic source, that is, $E = E_m + E_e$, $H = H_m + H_e$, for $[E_m, H_m]$ assuming that the current density is zero, and for $[E_e, H_e]$ magnetic flux density is assumed to be zero, so, $[E_m, H_m]$ satisfy the equation

$$\begin{aligned} \nabla \times E_m &= -J_m^s - \hat{z}H_m \\ \nabla \times H_m &= \hat{y}E_m \end{aligned} \quad (10)$$

And $[E_e, H_e]$ satisfy the equation:

$$\begin{aligned} \nabla \times E_e &= -\hat{z}H_e \\ \nabla \times H_e &= J_e^s + \hat{y}E_e \end{aligned} \quad (11)$$

Or $[E_m, H_m]$ is generated by the magnetic flux, and $[E_e, H_e]$ is generated by the current. The total field is the sum of two terms. Of Eqs. (10) with (11), take divergence, to give:

$$\begin{aligned}\nabla \cdot H_m &= -\frac{\nabla \cdot J_m^s}{\hat{z}} \\ \nabla \cdot E_m &= 0 \\ \nabla \cdot H_e &= 0 \\ \nabla \cdot E_e &= -\frac{\nabla \cdot J_e^s}{\hat{y}}\end{aligned}\quad (12)$$

From Eq. (12) it can be seen that there must be a function of two vectors, that is, a rotation of each of E_m and H_e :

$$\begin{aligned}E_m &= -\nabla \times F \\ H_e &= \nabla \times A\end{aligned}\quad (13)$$

Substituting Eq. (13) into Eq. (10) with Eq. (11) have

$$\begin{aligned}H_m &= -\hat{y}F - \nabla U \\ E_e &= \hat{z}A - \nabla V\end{aligned}\quad (14)$$

where U and V are two arbitrary scalar function newly introduced. With Eqs. (13) and (14), Eq. (10) becomes

$$\nabla \times \nabla \times F = J_m^s - \hat{y}zF - \hat{z}\nabla U\quad (15)$$

With Eqs. (13) and (14), Eq. (11) becomes:

$$\nabla \times \nabla \times A = J_e^s - \hat{y}zA - \hat{y}\nabla V\quad (16)$$

Expanded using vector function formula obtained for the two left formula

$$\begin{aligned}\nabla \nabla \cdot F - \nabla^2 F &= J_m^s - \hat{y}zF - \hat{z}\nabla U \\ \nabla \nabla \cdot A - \nabla^2 A &= J_e^s - \hat{y}zA - \hat{y}\nabla V\end{aligned}\quad (17)$$

Scalar U and V are arbitrary, U and V will be defined by the Lorentz computationally convenient conditions, that is,

$$\begin{aligned}\nabla \cdot F &= -\hat{z}U \\ \nabla \cdot A &= -\hat{y}V\end{aligned}\quad (18)$$

Thus, Eq. (17) is reduced to the non-simplified homogeneous Helmholtz equation of F and A :

$$\begin{aligned}\nabla^2 F + k^2 F &= -J_m^s \\ \nabla^2 A + k^2 A &= -J_e^s\end{aligned}\quad (19)$$

Suitable for containing the magnetic current source or current source region.

2.3. Boundary conditions

Solid electromagnetic geophysical problem is mainly involved in the action of current applied field (one field), the field strength or potential. Causing secondary primary field current and charge distribution, thereby generating the secondary field. The total field is the primary and secondary fields. Whether in one field or the second field at the same time satisfy Maxwell's equations or export equation, but also meet the appropriate boundary conditions. These boundary conditions are set in accordance with the nature of the problem in the partition boundary involved in a homogeneous medium (e.g., air interface with the earth) at.

The method to B : through medium 1 and medium 2 interface A, B of the normal component B_n is continuous, that is, $B_{n1} = B_{n2}$.

Normal to the D : at the interface of two media, since there is bulk density. The surface charge, D is the component discontinuous D_n , that is, $D_{n1} - D_{n2} = \rho_s$.

Tangential E : E_t tangential component when passing through the interface is continuous, that is, $E_{t1} = E_{t2}$.

Tangential H : if the current plane, to the absence of cut H_t component is continuous through the interface, that is, $H_{t1} = H_{t2}$.

Current density J : J_n normal to the component through the interface is continuous, that is, $J_{n1} = J_{n2}$.

Strictly speaking, this condition only applies to the case of DC, but ignoring displacement current, this condition may be applied.

Scalar potential: defined by the following equation static scalar potential V and U : $E = -\nabla V$, $H = -\nabla U$. Through the interface it is continuous, that is, $V_1 = V_2$, $U_1 = U_2$. Potential F : uniaxial symmetry, the interface perpendicular to the Z (perpendicular to the magnetic dipole layered earth) where, at the interface, the continuity conditions of the scalar potential are equivalent.

$$F_{z1} = F_{z2}, \quad \frac{1}{\mu_1} \frac{\partial F_{z1}}{\partial z} = \frac{1}{\mu_2} \frac{\partial F_{z2}}{\partial z}\quad (20)$$

Potential A : uniaxial symmetry, perpendicular to the Z -interface (electric dipole perpendicular to the layered earth) where, at the interface:

$$A_{s1} = A_{s2}, \quad \frac{1}{\hat{y}_1} \frac{\partial A_{s1}}{\partial z} = \frac{1}{\hat{y}_2} \frac{\partial A_{s2}}{\partial z}\quad (21)$$

3. Theoretical basis of simulation

3.1. Simulation of mathematical models

Emission provided on the ground, a circular receiving antenna [3–5], shown in Fig. 1, is equal to the frequency of the pulse current input antenna La Moer frequency excitation magnetic field is formed perpendicular to the B_0 magnetic excitation field vertical component $B_{1\perp}(r, \rho(R), a)$ that the proton magnetization M_0 (magnetization per unit volume of the sample is the sum of the statistical distribution of the nuclear magnetic moments) equilibrated positional deviation of the magnetic field direction at an angle θ :

$$\theta = 0.5\gamma B_{1\perp}(r, \rho(r), a)q \tag{22}$$

wherein the component is $B_{1\perp}$ excitation magnetic field perpendicular to the ground, $q = I_0^* \tau p$ called excitation pulse moments, I_0 and τp are the amplitude and duration of the current pulse, $r = r(x, y, z)$ is a vector of coordinates. It is the proton gyromagnetic ratio, wherein $\gamma = (2.675221 \pm 0.00000081) * 108 \text{ Am}^2/(\text{Js})$, a is the inclination of the geomagnetic field. Vector $M(r)$ about the earth's magnetic field at a frequency as La Moer Larmor precession.

When the pulse is terminated, the receiving antenna consisting of induced electromotive force $E(t, q)$, it indicates that the underground water [6] is present. among them:

$$E(t, q) = E_0(q) \exp(-t/T_m^*) \sin(\omega_0 t + \phi_0) \tag{23}$$

T_m^* is spin-spin relaxation time of NMR signals in MS, ϕ_0 is the initial phase of the NMR signal, a second phase shift relative to the excitation field current, in degrees, the initial amplitude $E_0(q)$ as:

$$E_0(q) = \omega_0 M_0 \int_v \beta_{1\perp} \sin\left(\frac{1}{2} \gamma \beta_{1\perp} q\right) n(r) dV(r) \tag{24}$$

among them, $\beta_{1\perp} = \beta_{1\perp} / I_0 = f(r, \rho(r), \alpha)$ referred to specific induction.

Vertical distribution assumed known horizontal earth layer, resistivity ($\rho(R) = \rho(Z)$), then (Eq. (24)) can be written as:

$$E_0(q) = \int_0^l K(q, \rho(z), \alpha, z) n(z) dz \tag{25}$$

where $K(q, \rho(z), \alpha, z) = \omega_0 M_0 \iint_{x,y} \beta_{1\perp}(z, \rho(z), \alpha) \sin\left(\frac{1}{2} \gamma \beta_{1\perp} q\right) dx dy$, $N(z) = VF/V$ is in ground water, $0 \leq n(z) \leq 1$, $q = I_0^* \tau p$, $dV = dx * dy * dz$, V_p , V are free water volume and the detection volume within the probe volume, $L = 2D$, D is the antenna diameter, the unit is m.

3.2. Calculation method of the NMR signal ground aquifer

Electrically conductive medium, the coil magnetic field and the magnitude and phase of the underground

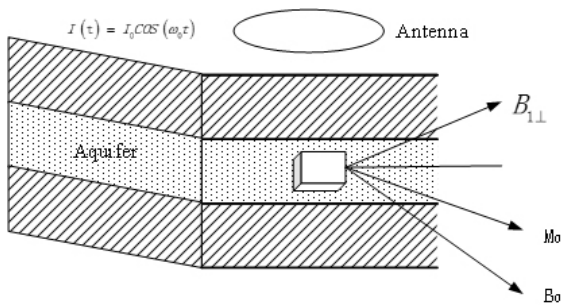


Fig. 1. NMR model for groundwater exploration.

nuclear magnetic change occurs due to the shielding effect of the conductance of the medium produced. Frequency domain electromagnetic field can be expressed in the form: $E \cdot e^{-j\omega t}$ with $H \cdot e^{-j\omega t}$ satisfy the Maxwell equation (Eq. (3)), the charge distribution in the region of the free surface is: $\nabla \cdot E = \nabla \cdot H = 0$.

To calculate the magnetic field coil and the NMR signal ground, approximately uniform half-space model can be used [6], a model of non-conductive medium in the air, the other the earth model comprising a conductive medium, in this case, considered normal electromagnetic fields. Lin et al. [7] calculated a first magnetic dipole field. Kirkland et al. [8] studied of the normal field annular current source. Suppose placed circular metal coil on the ground, placed on the cylindrical coordinate system r, ϕ, z . Then the surface coil position $z = 0$, $r = R_0$, R_0 is the radius of the coil. In $z > 0$ is a region (the entire subsurface region). Conductivity is $\sigma = \sigma_1$ uniform half-space. The conductivity of the surface of the air $\sigma_0 = 0$. Since the axisymmetric magnetic field is present only in the vertical component. In $z > 0$ half-space, the magnetic field derived from the solution of Maxwell's equations coils have the following form:

$$\begin{aligned} H_{1z}(r) &= IR_0 \int_0^\infty \frac{m^2}{m+u} e^{-uz} J_1(R_0 m) \cdot J_0(rm) dm \\ H_{1r}(r) &= IR_0 \int_0^\infty \frac{mu}{m+u} e^{-uz} J_1(R_0 m) \cdot J_1(rm) dm \end{aligned} \tag{26}$$

Here $u = (m^2 - \epsilon\mu\omega^2 - i\sigma\mu\omega)^{1/2}$, J as a Bessel function. Excitation field $H_1(r) \cdot e^{-i\omega t}$ can be seen as a plural. NMR signal is also a complex number having a phase and amplitude.

Formula can calculate the magnetic field at any subterranean aquifers by, after the magnetic field is brought into the equation (Eq. (24)) to obtain a signal ground aquifer NMR [9–10].

3.3. Calculation of the NMR signal ground aquifer two

Calculated using the simplified model shown in Fig. 2, this model assumes that:

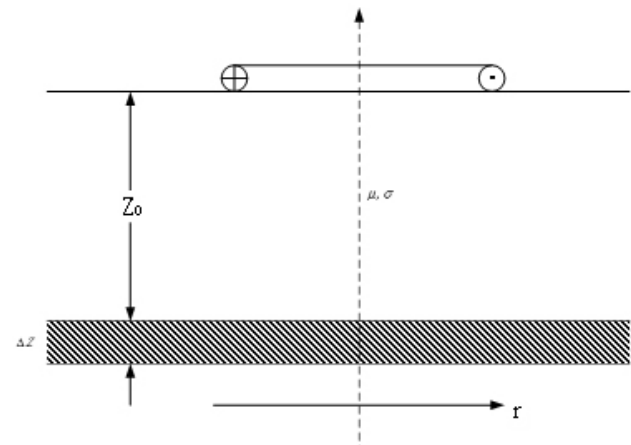


Fig. 2. Simplified model for computing.

Surface coils can form a magnetic moment M , as a step function of time with [11], which is: $M(t) = \begin{cases} 0(t > 0) \\ M(t < 0) \end{cases}$.

Size of the aquifer to the coil is small compared with the distance, that is, $D \ll Z_0$.

This magnetic field is perpendicular to the mainland range (field with axial symmetry, M being located at the surface of the magnetic moment of the magnetic dipole).

The conductive layer is located between the surface and an aqueous layer, in this case, the influence of the conductive layer aquifer NMR signal should be obvious.

Using the principle of reciprocity method commonly used in electrical prospecting, solving the NMR signal aquifer.

Time-domain homogeneous half-space model substantially Maxwell equations can be expressed as Eq. (1) wherein the free surface of the surface charge region still expressed as: $\nabla \cdot E = \nabla \cdot H = 0$

Using a cylindrical coordinate system (r, ϕ, z) , the magnetic flux density and electric field intensity in the time domain is expressed as:

$$\begin{aligned} \frac{\partial B_z^{(0)}(t)}{\partial(t)} &= \frac{1}{r} \frac{\partial}{\partial r} r E_\phi(r, z, t) \\ \frac{\partial B_r^{(0)}(t)}{\partial(t)} &= \frac{\partial}{\partial z} E_\phi(r, z, t) \end{aligned} \quad (27)$$

Introducing two auxiliary functions f_1, f_2 , the electric field intensity may be expressed as:

$$\begin{aligned} E_\phi &= \frac{4Mr}{\pi\sigma R^5} \int_0^{u_R^2} e^{-x} f_1(x) dx + \frac{4M}{\pi\sigma r^3 z} \int_0^{u_s^2} e^{-x} f_2(x) dx \\ R^2 = r^2 + z^2, \quad u_R^2 &= \mu\sigma R^2/4t, \quad u_s^2 = \mu\sigma z^2/4t \end{aligned} \quad (28)$$

among them,

$$\begin{aligned} f_1 &= \frac{x^{3/2}}{2\sqrt{\pi}} \left(1 - 2x \frac{z^2}{R^2} \right) \\ f_2 &= \frac{x^2 r^2}{2z^4} \exp\left(-\frac{xr^2}{2z^2}\right) \left\{ \left(\frac{3}{2} - \frac{xr^2}{z^2} \right) I_0\left(\frac{xr^2}{2z^2}\right) + \left(\frac{xr^2}{z^2} - \frac{1}{2} \right) I_1\left(\frac{xr^2}{2z^2}\right) \right\} \end{aligned}$$

Using the conversion relationship between the time and frequency domains: $E_\phi(r, z, \omega) = \int_0^\infty e^{-i\omega t} E_\phi(r, z, t) dt$, the electric field intensity in the form of a time domain a frequency domain representation is rewritten as appropriate:

$$\begin{aligned} E_\phi(r, z, \omega) &= \frac{4Mr}{\pi\sigma R^5} \int_0^\infty \frac{1 - \exp\left(-i\omega \frac{\mu\sigma R^2}{4x}\right)}{i\omega} e^{-x} f_1(x) dx \\ &+ \frac{4M}{\pi\sigma r^3} \int_0^\infty \frac{1 - \exp\left(-i\omega \frac{\mu\sigma z^2}{4x}\right)}{i\omega} e^{-x} f_2(x) dx \end{aligned} \quad (29)$$

At low frequencies, taking $\omega \rightarrow 0$, the above equation is further simplified as: $E_\phi(r, z, \omega) = \frac{Mr\mu}{4\pi R^5} - i\omega \frac{\mu^2\sigma M}{16\pi} \left(\frac{r^3}{R^3} + \frac{z}{r} + \frac{z^4}{rR^3} \right)$.

(27) Z is differentiated to obtain a magnetic flux density which is calculated as follows:

$$\begin{aligned} B_r^{(0)}(\omega) &= -\frac{3\mu Mrz}{4\pi R^5} \\ &+ i\omega \frac{\mu^2\sigma M}{16\pi} \left(\frac{3zr^3}{R^5} - \frac{1}{r} + \frac{4z^3}{R^3 r} - \frac{3z^5}{rR^5} \right) \end{aligned} \quad (30)$$

After the last projection, Z_0 of depth, the initial thickness of the NMR signal amplitude of the aqueous layer is ΔZ :

$$E_0 q = \frac{3\mu\omega_0 M_0 s \Delta Z n}{2Z} |U(p)| \quad (31)$$

For any ω , Eq. (28) obtained by differentiating the electric field strength on the z formula: $B_r^{(0)}(\omega) = B_r^1(\omega) + B_r^2(\omega)$, the following formula exploded form two addends:

$$\begin{aligned} B_r^{(1)} &= -\frac{45Mrz}{2i\omega\pi\sigma R^7} \left\{ 1 - e^{-y} \left(1 + y + \frac{2}{5}y^2 + \frac{1}{15}y^3 \right) \right\} \\ &+ \frac{105Mrz^3}{2i\omega\pi\sigma R^9} \left\{ 1 - e^{-y} \left(1 + y + \frac{3}{7}y^2 + \frac{12}{21}y^3 + \frac{1}{105}y^4 \right) \right\} \\ B_r^{(2)} &= \frac{4Mr}{\pi^2\sigma} \int_0^\pi \frac{d\theta}{i\omega} \left\{ \begin{aligned} &\left[\frac{\frac{3}{2} - \frac{1}{2}\cos\theta}{\rho^6} \left(1 - \Phi_3\left(y \frac{\rho}{R}\right) \right) \right. \\ &+ \frac{3z^2(\cos\theta - 3) + 3r^2(\cos\theta - 1)}{\rho^8} \\ &\left. \left(1 - \Phi_4\left(y \frac{\rho}{R}\right) \right) \right] \\ &+ \frac{24z^2 r^2 (1 - \cos\theta)}{\rho^{10}} \\ &\left. \left(1 - \Phi_5\left(y \frac{\rho}{R}\right) \right) \right] \end{aligned} \right\} \end{aligned} \quad (32)$$

Complex quantity $U(p)$ represented by the formula:

$$U(p) = \text{Re}U + \text{Im}U = \int_0^\infty |b| e^{i\theta_0} \sin(|b|p) g \cdot dg \quad (33)$$

where $g = r/Z_0$, complex function $b(g) = |b| e^{i\theta_0}$, which was expressed as:

$$\begin{aligned} b(g) &= \frac{g}{(g^2 + 1)^{5/2}} \\ &- \frac{i\lambda}{12} \left[\frac{3g^3}{(g^2 + 1)^{5/2}} - \frac{1}{g} + \frac{4}{g(g^2 + 1)^{3/2}} - \frac{3}{g(g^2 + 1)^{5/2}} \right] \end{aligned} \quad (34)$$

4. Numerical simulation and analysis of factors

As it can be seen from the above equation, in the calculation of the NMR signal, first calculation and analysis of $U(p)$ and $b(g)$ function, using the latest software MAPLE above mathematical function $U(p)$ and $b(g)$ direct numerical integration, in order to ensure the accuracy in calculating the preparation of using the program accumulation mode, $b(g)$ when θ integration of expression, is solved by the following equation:

$$\frac{1}{\pi} \int_0^\pi f(\cos \theta) d\theta = \frac{1}{N} \sum_{i=1}^N f \cos \theta_i \tag{35}$$

where $\theta_i = \frac{(2i-1)\pi}{2N}$.

To ensure the accuracy of order N , in the preparation of the program taken as $N = 100$. of $U(p)$ parabolic integral equation:

$$U = \frac{0.1 \left(f(0) + 2 \left(\sum_{i=1}^{14} f(0.2i) \right) + 4 \left(\sum_{i=0}^{14} f(0.1(2i+1)) \right) + f(3) \right)}{6} \tag{36}$$

4.1. Simulation results analysis

$|U(p)|$ with a function curve shown in Fig. 3 by: $p = 3S\gamma q\mu / 8\pi Z_0^3$ known, when the depth of the aquifer Z_0 is constant, p is the excitation pulse with $q = I_0 \cdot \tau p$ moment proportional to the parameters, from the graph (a) $\lambda = 0$, (b) $\lambda = 5$ known, when $\lambda = 0$ when, that is, the non-conductive overburden aquifer, the $U(p)$ into a linear relationship, $p = 7.5$ when the maximum value is reached. p -value increases as can be seen $|U(p)|$ slow decay and a weak shock, reflecting spin signals having different phases with the radial coordinate competitive contribution $g = r/Z_0$ of. With the increasing value of λ , that is, conductivity enhancement, $|U(p)|$ of the amplitude is gradually decreased, and $|U(p)|$ is the magnitude of the first maximum value position is increased in the direction p mobile.

The aqueous layer depth is constant $E_0(q)$ with the function q curve in Fig. 4. By analysis of $b(g)$ function, and $U(p)$ function, can be taken to ensure the accuracy $0 \leq \lambda \leq 10$ integral taken within this range $\lambda = 0, \lambda = 5$ several E_0 to obtain a set of (q) with q function curve, the curve can be seen from this set, when a certain depth and thickness of the aquifer, λ . Since a uniform half-space medium conductivity increases, so that E_0-q curve shape of the NMR signal changes, that is, when λ from small change to large, that is, the conductive medium becomes good, a first maximum value E_0-q on the curve from

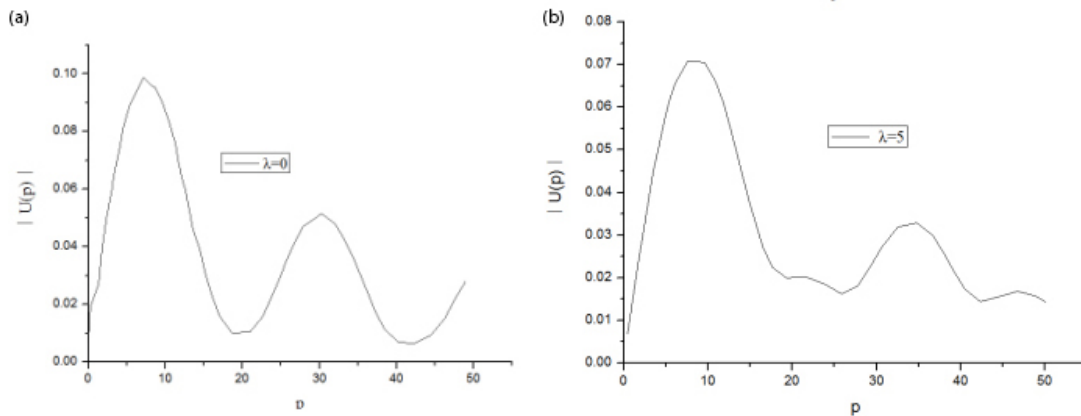


Fig. 3. Aquifer depth changes, conductive $U(P)$, with the change of p-function curve. (a) When conductive $U(P)$, with the change of p-function curve. (b) When conductive $U(P)$ with the change of p-function curve.

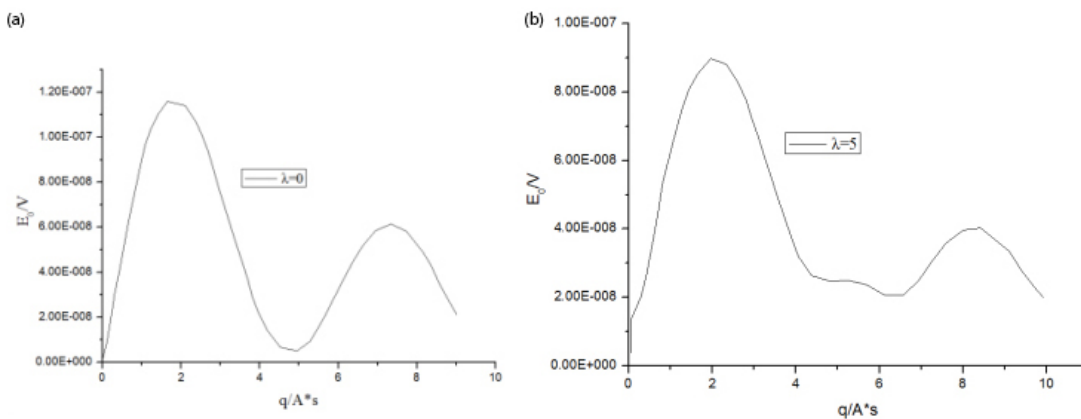


Fig. 4. E_0-q curves of electrical conductivity change. (a) When E_0-q curves of electrical conductivity change. (b) When E_0-q curves of electrical conductivity change.

large to small. When $\lambda = 0$, q is approximately $2 \text{ A}\cdot\text{s}$ when the initial amplitude $E_0(q) = 1.2 \cdot 10^{-7} \text{ V}$; when $\lambda = 5$, q is about $2.5 \text{ A}\cdot\text{s}$ when the initial amplitude $E_0(q) = 8.8 \cdot 10^{-8} \text{ V}$, that is, $E_0(q)$ a first maximum value is moved to the position q increasing direction, and the initial amplitude attenuated with enhanced conductivity.

4.2. Effect of changes in the moisture content of the NMR signal aquifer

Groundwater quantitative interpretation of the content: a total volume V is set to detect the ground, and V_w is the total volume of the aqueous portion of the volume, the VR is the volume occupied by underground rock, then we can write the following equation:

$$V = V_w + \text{VR} \tag{37}$$

Suppose water and rock (VR) is isotropic and homogeneous distribution of the total volume, the total volume of the ground can be replaced with a unit volume ($V = 1 \text{ m}^3$). Volume of water (and V_w) in the porous medium can be divided into two parts: the free water volume VF (this water is independent of the presence of the rock particles can be extracted out) and bound water volume VB (which portion of the water is covered with the rock among the particles cannot be extracted), it is assumed $V_w = \text{VF} + \text{VB}$. Two portions of water and free water to bound water mechanically explained by relaxation time. NMR relaxation signal is substantially different, wherein the relaxation time of the bound water is very short. Although further studies have to accurately estimate the relationship between the hydrogeological parameters and relaxation times of the NMR signal porous media needs, NMR method in water experience allows for assuming: relaxation time T_2 * bound water less than $20\text{--}30 \text{ ms}$, and the relaxation time of free water $30 \text{ ms} \leq T_2 \leq 1,000 \text{ ms}$. NMR equipment currently used, for example, looking for water NUMIS (IRIS Instruments, France) instrument is set dead time cannot be less than 30 ms detection signal, it can be described only in the formation of free water VF NMR signal to be detectable. Thus defining free water content percentage of the total volume of water, written as: $n(z) = \text{VF}/V$, $0 \leq n(z) \leq 1$, for example, in a dry rock: $n(z) = 0$, and in overall water $n(z) = 1$ lake.

When the coil parameters unchanged, the aqueous layer is proportional to the water content and the NMR signal amplitude. Taken Larmor frequency of $2,385 \text{ Hz}$, the aqueous layer disposed over the resistance of medium $\rho_{10} = \Omega \text{ m}$, select the radius of the circular coil 50 m , the depth of the aquifer 50 m , a thickness of 10 m , respectively, when the calculated moisture content of 10% , $E_0\text{-}q$ 40% curve in Fig. 5. The morphological changes seen from the curve:

Description: when the coil constant parameters, water content and the aqueous layer are proportional to the amplitude of the NMR signal, when the level of the water content of the aqueous layer is gradually increased, the position where the amplitude $E_0\text{-}q$ curve does not change, indicating at the same depth exploration aqueous layer excitation pulses required torque value is constant, but the amplitude of the aquifer water content is increased such that $E_0\text{-}q$ curve significantly larger; aquifer water content that is greater the amplitude

of the measured NMR signal to the larger, which is the best embodiment of the water directly to the NMR method.

4.3. Effect of the coil area of the NMR signal variation

From Eq. (31), it can be seen that the size of the antenna area is directly proportional to the amplitude of the NMR signal. Taken Larmor frequency of $2,385 \text{ Hz}$, the aqueous layer depth is set 50 m , the aqueous layer having a thickness of 10 m , an aqueous layer over the dielectric resistivity of $\rho = 10 \Omega \text{ m}$, transmitting, receiving antennas $E_0\text{-}q$ curve radius is calculated as follows 30 m (Fig. 6). From the graph of the change of shape, when the radius of 30 m ($S = 2,826 \text{ m}^2$) to be probed 50m , 10m thick deep aquifers at least a desired pulse torque value $q = 10 \text{ A}\cdot\text{s}$, the antenna radius 40 m ($S = 5,024 \text{ m}^2$) is detecting 50m , 10m deep aquifer thickness required to achieve a desired pulse torque value $q = 6.8 \text{ A}\cdot\text{s}$, when the antenna radius of 50 m ($S = 7,850 \text{ m}^2$), detecting a thickness of 10m , 50m deep aquifer is simply rectangular pulse $q = 4 \text{ A}\cdot\text{s}$ can.

Note: For the case where only a horizontal underground aquifer, when the transmitting and receiving antenna area is increased, the excitation pulse moment exploration same aquifer depth and thickness required is reduced, and the antenna area is increased, the same the aqueous layer depth and thickness of the NMR signal amplitude significantly increased.

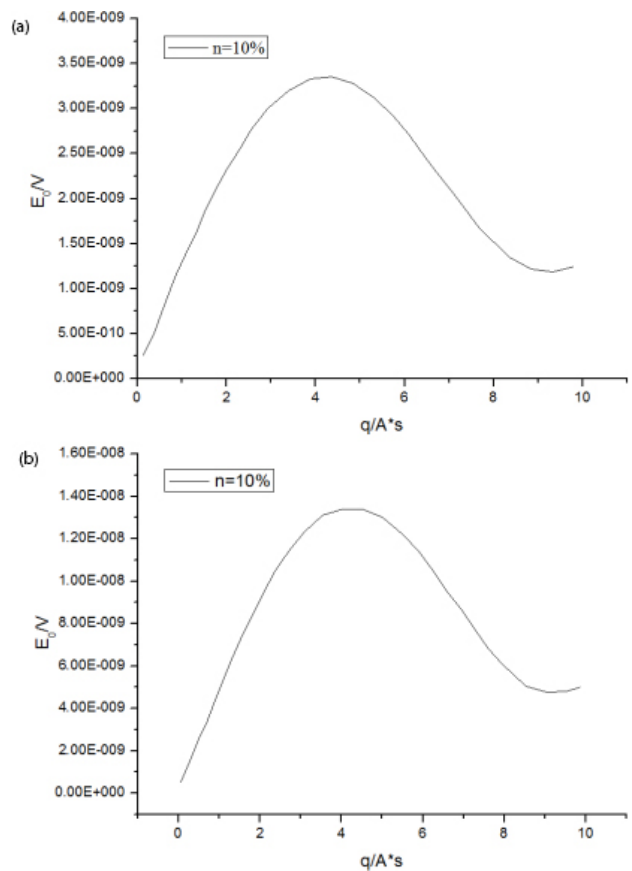


Fig. 5. $E_0\text{-}q$ curves of water content variation in horizontal aquifers in homogeneous half-space. (a) When $n = 10\%$, $E_0\text{-}q$ curves. (b) When $n = 40\%$, $E_0\text{-}q$ curves.

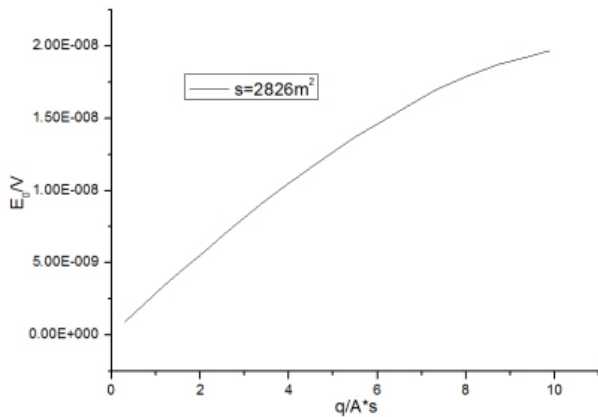


Fig. 6. E_0 - q curve when the antenna area changes in a half-space horizontal aquifer.

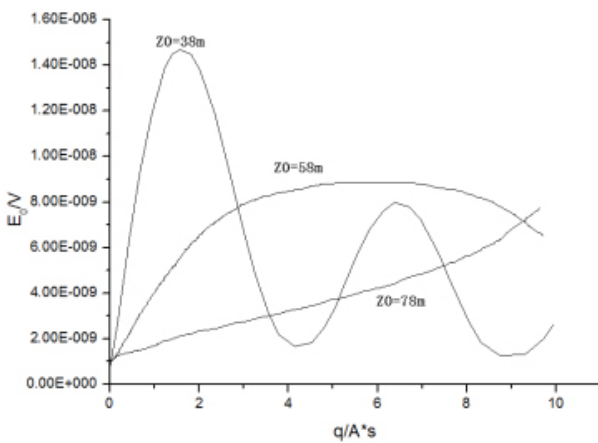


Fig. 7. E_0 - q curves of horizontal aquifer depth variation in a uniform half-space.

4.4. Aqueous layer depth variations affect the NMR signal

From Eq. (31) it was found that the depth is inversely proportional to the size of the NMR signal amplitude level of the aqueous layer. Taken Larmor frequency of 2,385 Hz, the aqueous layer having a thickness of 10 m, the water content of $n = 9\%$, resistivity of the dielectric layer above the aqueous $\rho = 10 \Omega \text{ m}$, transmitting, receiving antenna area is $S = 12,740 \text{ m}^2$, exploration depth was taken as $Z_0 = 38 \text{ m}$, $Z_0 = 58 \text{ m}$, E_0 - q curve $Z_0 = 78 \text{ m}$ obtained by the simulation shown in Fig. 7, the curve shape can be learned: the aqueous layer depth increases NMR signal amplitude decreases, and with increasing depth of the aquifer, the excitation pulse moment required value will also increase, which also shows the probed under the same conditions the area of the antenna depth the aqueous layer is necessary to increase the moment of excitation pulses, and 78 m deep aquifers $q = 5 \text{ A*s}$ when the amplitude has not occurred, indicating undetectable 78 m deep aquifer.

5. Conclusion

A single horizontal aquifer simulation model of layered earth is established in this paper. The simulation calculation of the model is carried out in consideration of the influence of the conductivity of the medium on the water content,

the water content in the aquifer and the depth of the aquifer. The simulation results show that the conductivity of the medium above the aquifer will affect the exploration depth of the NMR water finding method. The good conductive layer above the aquifer will lead to the decrease of the exploration depth. The water content in the aquifer is proportional to the amplitude of the NMR signal. The greater the water content of the underground aquifer is, the greater the amplitude of the measured NMR signal is. It indicates that the greater the water content of the aquifer is, the easier it is to be detected. This is the best embodiment of using the NMR method to find water directly.

Acknowledgements

This work is supported by the Yangtze Youth Fund, No 2015cqjn31 and Open Fund of Key Laboratory of Exploration Technologies for Oil and Gas Resources (Yangtze University), Ministry of Education (No K2016-15 and No K2016-14).

References

- [1] E. Grunewald, D. Grombacher, D.O. Walsh, Adiabatic pulses enhance speed and sensitivity of geophysical surface NMR measurements for groundwater investigations, ASEG Extended Abstracts, 2015 (2015) 1–3.
- [2] M. Born, E. Wolf, Principles of Optics: Electromagnetic Theory of Propagation, Interference and Diffraction of Light, Cambridge University Press, London, 2013.
- [3] J. Pan, Z. Li, Y. Zhang, J. Bernard, L. Chen, L. Gao, M. Xie, Correlating intensity of pulse moment with exploration depth in surface NMR, J. Appl. Geophys., 142 (2017) 1–13.
- [4] R. Knight, D.O. Walsh, J.J. Butler, E. Grunewald, G. Liu, A.D. Parsekian, M. Barrows, NMR logging to estimate hydraulic conductivity in unconsolidated aquifers, Groundwater, 54 (2016) 104–114.
- [5] L. Chavez, S. Altobelli, E. Fukushima, T. Zhang, T. Nedwed, D. Palandro, H. Thomann, Detecting Arctic oil spills with NMR: a feasibility study, Near Surf. Geophys., 13 (2015) 409–416.
- [6] A.D. Parsekian, K. Dlubac, E. Grunewald, J.J. Butler, R. Knight, D.O. Walsh, Bootstrap calibration and uncertainty estimation of downhole NMR hydraulic conductivity estimates in an unconsolidated aquifer, Groundwater, 53 (2015) 111–121.
- [7] J. Lin, Y. Zhang, Y. Yang, Y. Sun, T. Lin, Anti-saturation system for surface nuclear magnetic resonance in efficient groundwater detection, Rev. Sci. Instrum., 88 (2017) 064702.
- [8] C.M. Kirkland, R. Hiebert, A. Phillips, E. Grunewald, D.O. Walsh, J.D. Seymour, S.L. Codd, Biofilm detection in a model well-bore environment using low-field NMR, Groundwater Monit. Remed., 35 (2015) 36–44.
- [9] K.P. Tan, R.S. Brodie, L. Halas, K. Lawrie, Using airborne EM and borehole NMR data to map the transmissivity of a shallow semi-confined aquifer, western NSW, ASEG Extended Abstracts, 2015 (2015) 1–4.
- [10] P. Höhener, Z.M. Li, M. Julien, P. Nun, R.J. Robins, G.S. Remaud, Simulating Stable Isotope Ratios in Plumes of Groundwater Pollutants with BIOSCREEN-AT-ISO, Groundwater, 55 (2017) 261–267.
- [11] P.J. Hawke, A. Harrild, E. Grunewald, Determination of Formation Specific NMR Calibrations for Water Well Evaluation in a Semi-Consolidated Aquifer, ASEG Extended Abstracts, 2016 (2016) 1–5.